Experimental demonstration of the Rayleigh acoustic viscous boundary layer theory

J. R. Castrejón-Pita,* A. A. Castrejón-Pita,† G. Huelsz, and R. Tovar
Centro de Investigación en Energía, UNAM A. P. 34, 62580 Temixco, Morelos, Mexico
(Received 19 August 2005; published 2 March 2006)

Amplitude and phase velocity measurements on the laminar oscillatory viscous boundary layer produced by acoustic waves are presented. The measurements were carried out in acoustic standing waves in air with frequencies of 68.5 and 114.5 Hz using laser Doppler anemometry and particle image velocimetry. The results obtained by these two techniques are in good agreement with the predictions made by the Rayleigh viscous boundary layer theory and confirm the existence of a local maximum of the velocity amplitude and its expected location.

DOI: 10.1103/PhysRevE.73.036601 PACS number(s): 43.58.+z, 43.20.+g, 47.15.Cb

I. INTRODUCTION

The phenomenon involved in the acoustic boundary layer was originally studied by Rayleigh in the nineteenth century [1]. Since then, this phenomenon has been extensively studied by many authors, Westervelt [2], Nyborg [3], Lighthill [4], and Qi [5], among others, see a review in [6]. Recently, these studies have regained importance motivated by their applications in the thermoacoustic effect [7], and gyrometryacoustic and acoustic streaming [8,9].

The presence of rigid bodies modifies the oscillatory flow intrinsic in an acoustic wave to fulfill the condition of zero relative velocity at the fluid-solid interface. This manifests the fact that in the region near the wall, namely, in the boundary layer, dissipative effects can not be ignored. It is precisely the existence of dissipation, which can induce an effective transport in oscillatory boundary layers even in zero-mean flow. These modifications are characterized by the changes in amplitude and phase of the velocity relative to their values far away from the wall.

Measurements of the oscillatory velocity in the laminar acoustic viscous boundary layer (LAVBL) are difficult to perform. Instruments must be sensitive enough to measure very small velocity amplitudes, with enough temporal resolution to solve the wave frequency and the velocity phase relative to the pressure, and with enough spatial resolution to solve the structure of the boundary layer which is confined to a small region near the wall. For example, in an acoustic wave in air at room conditions with a wave frequency of 70 Hz and 100 Pa, the amplitude of the velocity oscillations goes from 0.25 to 0 m/s in a boundary layer of approximately 1 mm. The width of the boundary layer decreases its value with increasing frequency. Due to these requirements, measurements in the LAVBL are scarce. Hino *et al.* [10] in 1976 used hot wire anemometry (HWA) for measurements in air oscillations produced by a piston with a frequency of 0.167 Hz. Their results show deviations from the theoretical predictions made by Rayleigh [1] of less than 20% for the velocity amplitude and 25% for the phase. Huelsz *et al.* [11], also using HWA, made measurements in the LABVL produced by acoustic standing waves of frequencies 35, 46, and 130 Hz in air. The values for the velocity amplitude agree with the theoretical predictions mentioned before with an error of less than 20% with a slight dependence on the frequency. However, the results for the phase show a stronger dependence on the phase with deviations of 7% for 130 Hz and 30% for 46 Hz.

In order to clarify whether these experimental and theoretical differences are intrinsic to the phenomenon or to the technique used, nonintrusive techniques, like laser Doppler anemometry (LDA) and particle image velocimetry (PIV), are used in the present study. The results show a good agreement between theory and the experimental data, less than 1% for LDA measurements and less than 3% for PIV.

The LDA and PIV are widely known techniques, complete descriptions of them can be found in [12]. Studies of boundary layers with LDA [13–15] and PIV [16–18] have been made recently. LDA has been used in acoustics [19,20] as well as PIV [21–24]. A review of LDA and PIV measurements in acoustic waves and acoustic streaming can be found in Ref. [25]. Nevertheless, no earlier work has been presented that reports amplitude and phase velocity measurements in the laminar acoustic viscous boundary layer with LDA nor with PIV.

II. THE RAYLEIGH THEORY

Rayleigh derived expressions for the first-order axial u^* and transverse v^* velocity components of an acoustic standing wave between two parallel plates separated by a distance $2y_w^*$. The superscript * is used for dimensional variables. He considered that $\delta_v \ll 2y_w^* \ll \lambda^*$, where λ^* is the wavelength and $\delta_v = \sqrt{2\mu^*/\rho^*\omega^*}$ the viscous boundary layer depth. In this last expression μ^* and ρ^* are the dynamic viscosity and the density of air, and $\omega^* = 2\pi f^*$ is the angular frequency with f^* being the frequency. Dimensionless quantities are defined as $y = y^*/\delta_v$ and $u = u^*/u_\infty$, where u_∞ is the transverse velocity far from the wall. Dimensionless time t is defined as $t = t^*/\omega^*$. Rayleigh showed that

$$u = \{1 - \exp[-(1+i)y]\}e^{it}. \quad (1)$$

*Present address: The Blackett Laboratory, Imperial College, Prince Consort Road, London SW7 2BZ, United Kingdom.

†Present address: Clarendon Laboratory, University of Oxford, Parks Road, Oxford OX1 3PU, United Kingdom.

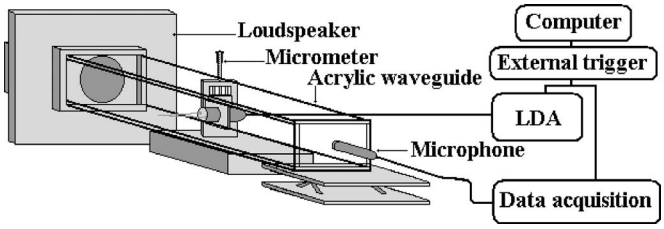

FIG. 1. Schematic view of the setup used for the study of the LAVBL using LDA.

A detailed derivation of this expression can be found in [1]. It can be seen from Eq. (1) that the axial velocity predicted by Rayleigh is independent of the frequency when it is written in dimensionless variables. However, experimental results obtained using HWA have shown a noticeable dependence on the acoustic wave frequency [11]. Although Tominaga ([26]) derived an expression without the restriction of the separation distance of the plates, for the experimental setup used in [11] ($2y_w^*=0.054$ m) and the range of frequencies studied, the differences in the LAVBL structure predicted by both theories are less than 0.01% and the dependence on frequency is unnoticeable.

III. EXPERIMENTAL SETUP

The experimental setup is shown schematically in Fig. 1. It essentially consisted of a waveguide, a sound wave system, a pressure measurement system, and a LDA or a PIV depending on the measurements carried out. Except for the last components, this setup was similar to the one used for the HWA measurements in [11].

Two different waveguides were used, both of rectangular cross sections of 0.098 m $\times$ 0.054 m, and with lengths of 0.60 m and 1.2 m in order to maintain quarter-wavelength standing waves of 114.5$\pm$0.1 Hz and 68.5$\pm$0.5 Hz, respectively. The waveguides were made of transparent acrylic to allow optical access. At one end of the waveguide was a loudspeaker and the other end was closed with a massive cap. The sound wave system consisted of a loudspeaker and a function generator (Wavetek model 29) connected to the loudspeaker via an amplifier (Onkyo model PI Integra with THD $\leqslant$0.001).

Pressure oscillations were measured with a microphone (Brüel & Kjaer model 2610) and an amplifier coupled to a data acquisition system (HP 3852A) controlled from a PC. The microphone was mounted into the cap where the pressure antinode was located. For synchronization purpose a function generator (Stanford Research model DS345) was used.

The LDA system consisted of a backscatter probe (Dantec FiberFlow 60 $\times$ 20), a photomultiplier, a Burst Spectrum Analyzer (Dantec BSA 57N11), an argon laser (Spectra Physics model 177) using the 488 nm line (100 mW), and a PC with the Dantec BSA Flow Software. This system allowed a measurement volume of 0.64 mm $\times$ 0.075 mm $\times$ 0.075 mm. For its displacement in the y direction, the LDA probe was set into a positioning system with a precision of 1 μm.

The PIV system used consists of a digital camera (Kodak 1.0 Megaplus/30 Hz with resolution of 1 Mpixels), two Nd-YAG lasers (1 J each), a synchronizer and a Processor (Dantec 1100 FlowMap), and a PC with the Dantec Flow Manager Software. The width of the laser beam has been estimated as 1 mm. It was used directly without the usual cylindrical lens to create a sheet. Coupled to the digital camera, a microscope was used (Infinity InfiniVarCFM with zoom, 100$\times$). Both systems, LDA and PIV, were located at an independent motion free base to prevent oscillations that could alter the experimental data.

The air inside the waveguide was at atmospheric pressure and at 23$\pm$1 °C. For LDA and PIV different types of seeding particles were tried and *Artemisa vulgaris* smoke was selected because it produces a sufficient number of particles, they remain suspended longer, have minimal drag, produce a minimal standard deviation on the velocity data because the size of the particles is more uniform than the other types of particles tried and they do not interact each other nor with the waveguide walls [27]. The typical aerodynamic diameter of this kind of smoke is 1.6 μm [28]. Measurements of the pressure amplitude and the resonance frequency were carried out with and without smoke particles and no changes were found.

Measurements were taken approximately 5 min after the smoke was injected and the function generator was turned on. Each experiment consists of a set of simultaneously initialized measurements of pressure and velocity in order to obtain the phase difference between them. In each measurement 10^4 microphone data were taken at a rate of 10^5 Hz. Measurements were done with pressure amplitudes in the range of 75 to 300 Pa. The data acquisition and its processing are particular for the LDA and PIV. They are independently presented in the next two sections.

IV. LDA DATA ACQUISITION AND PROCESSING

The LDA was used to measure the axial component of the velocity. The transversal size of the measurement volume was 0.075 mm, which is $0.28\delta_v$ for $f^*=68.5$ Hz and $0.36\delta_v$ for $f^*=114.5$ Hz. As LDA measurements give information of the velocity at a point (the center of the measurement volume), to obtain the velocity as a function of the transverse position (measured from the wall), y^*, different measurements have to be taken varying the LDA probe position. In each measurement 2×10^3 LDA data were acquired. Due to the characteristics of the LDA technique, the data are not equally spaced in time. In all experiments, the mean data rate outside of the LAVBL was greater than 10^3 Hz. This value decreases with the distance to the wall, limiting the minimum distance where mean data rate is enough for processing.

The synchronization between the LDA and the microphone signal was achieved using a square signal as trigger (5 V during 0.01 s and 0 V during 1 s). This signal was connected to the Burst Spectrum Analyzer external synchronization input and to the data acquisition system where the pressure measurements were taken. In the LDA system, the trigger in fact does not initialize the acquisition process be-

cause this is determined by the presence of particles in the measurement volume and this is a random process. However, using this method, the arrival of the trigger is recorded into the LDA synchronization status and the relative initial time is thus determined.

Velocity data from LDA were processed using three procedures: the first one consists of a data interpolation (constant or linear) for an equal time resampling and a fast Fourier transform (FFT) analysis, the second is a Lomb normalized periodogram [29], and in the third the data are accumulated into a single period and then a function fitting is applied. The first two procedures gave the acoustic wave frequency with a precision of ±0.1 Hz (the function generator precision was ±0.05 Hz), with differences in magnitude of less than 5%. In the third procedure the frequency f^* obtained from Lomb normalized periodogram was used to accumulate the data into a single period, and using a function fitting to $u=u_a^* \cos(2\pi f^* t^* - \Theta)$ the amplitude u_a^* and phase Θ were obtained. The difference between amplitude values from this last procedure and those using Lomb normalized periodogram was less than 0.1%.

From microphone output the amplitude and phase of the pressure at the antinode were calculated using the FFT. Using these values and the relationship for standing waves in adiabatic conditions, the amplitude and phase of the velocity outside the LAVBL were calculated. This amplitude value $u_{a\infty}^*$ was used to find a dimensionless velocity amplitude obtained from the data fit $u_a=u_a^*/u_{a\infty}^*$. The calculated velocity phase was used to report the phase obtained from the LDA data fit relative to the phase outside the LAVBL.

V. PIV DATA ACQUISITION AND PROCESSING

The PIV system was used to measure the axial and transverse components of the velocity. For the cross correlation, interrogation areas of 128 pixels in the axial direction and 32 pixels in the transverse direction, were used. The measurement volume corresponding to each velocity data from PIV is determined by the interrogation area size and the width of the laser. For the setup used here, the measurement volume was $\approx 0.124\ \text{mm} \times 0.031\ \text{mm} \times 1\ \text{mm}$; thus in the transverse direction y^* the spatial resolution corresponds to $0.11\delta_v$ for $f^*=68.5$ Hz and $0.15\delta_v$ for $f^*=114.5$ Hz. The acoustic wave frequencies were commensurable to the vector map acquisition frequencies, thus only seven vector maps were analyzed for 68.5 Hz and 9 for 114.5 Hz.

For all measurements the transverse velocity component was less than 0.01% of the axial component. Axial velocity data for each transverse position y^* were processed using a function fitting to $u=u_a^* \cos(2\pi f^* t^* - \Theta)$, amplitude u_a^*, frequency f^*, and phase Θ were obtained from the fitting. This procedure gave the acoustic wave frequency with a precision of ±0.1 Hz. As opposed to the LDA, the synchronization of the PIV and the microphone signal can be carried out using a typical transistor-transistor logic (TTL) trigger because this system can be initialized at will. The microphone signal was processed using the same procedure described in the previous section.

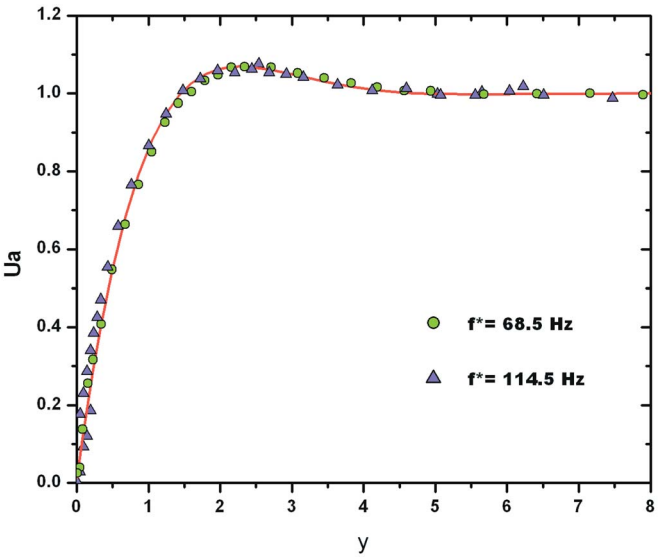

FIG. 2. (Color online) Dimensionless amplitude of the velocity oscillation as a function of the dimensionless distance to the wall. Symbols obtained by LDA measurements, line from Rayleigh theory.

VI. RESULTS AND DISCUSSION

The structure of the laminar oscillatory viscous boundary layer produced by acoustic waves is found by plotting the dimensionless amplitude of the velocity oscillation $u_a=u_a^*/u_{a\infty}^*$ and the phase of the velocity oscillation relative to its value far away from the wall α, as functions of the dimensionless distance to the wall $y=y^*/\delta_v$, $\delta_v=0.27$ mm and 0.21 mm, for 68.5 Hz and 114.5 Hz, respectively.

The results for the LDA measurements, obtained from the accumulated data, are shown in Figs. 2 and 3 together with theoretical predictions given by Eq. (1). For the measure-

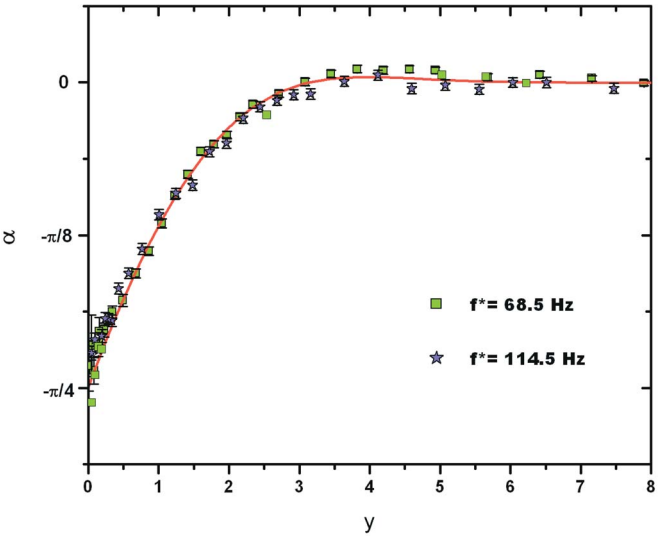

FIG. 3. (Color online) Phase of the velocity oscillation relative to its value far away from the wall as a function of the dimensionless distance to the wall. Symbols obtained by LDA measurements, line from Rayleigh theory.

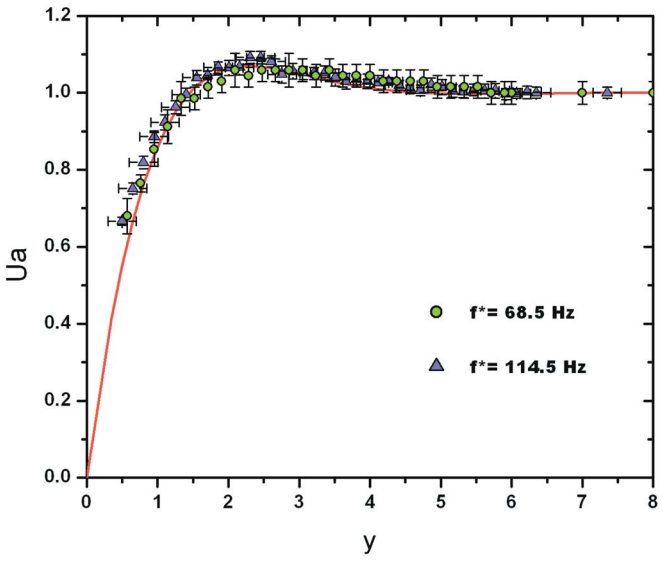

FIG. 4. (Color online) Dimensionless amplitude of the velocity oscillation as a function of the dimensionless distance to the wall. Symbols obtained by PIV measurements, line from Rayleigh theory.

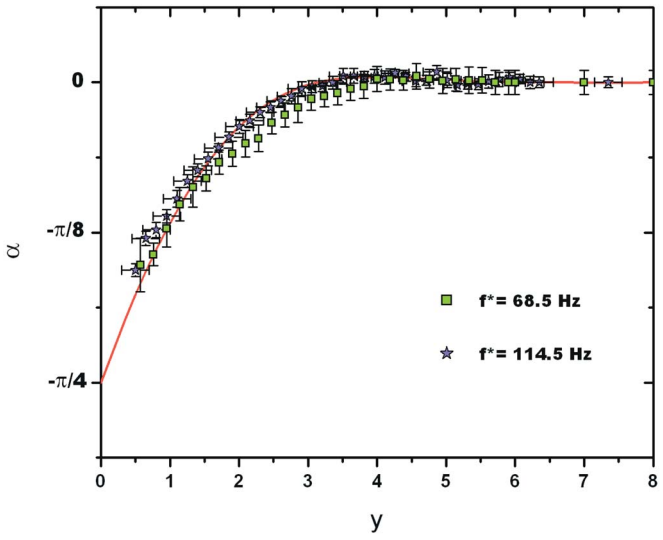

FIG. 5. (Color online) Phase of the velocity oscillation relative to its value far away from the wall as a function of the dimensionless distance to the wall. Symbols obtained by PIV measurements, line from Rayleigh theory.

ments close to the wall ($y<0.28\delta_v$ for $f^*=68.5$ Hz and $y<0.36\delta_v$ for $f^*=114.5$ Hz), a part of the measurement volume was lost within the acrilic wall but that does not stop the collection of data because the interference pattern still exists in the remaining volume and thus scattered light from particles can still be collected. The experimental uncertainty is of the order of the symbols size. Amplitude results from the other methods are similar. However, phase results are not equally effective, the other procedures have greater dispersion, up to 30% in the case of the Lomb periodogram.

PIV measurements are presented in Figs. 4 and 5 together with theoretical predictions given by Eq. (1).

All the experiments were performed in the laminar regime. The Reynolds number Re based on the velocity amplitude outside the boundary layer is defined by $\mathrm{Re}=u^*_{a\infty}\delta_v\rho^*/\mu^*$. In the experiments, Re is much smaller than the critical Reynolds number for turbulence [30].

The experimental results obtained with LDA and PIV measurements agree with theoretical results. For LDA, differences are less than 1% for $y\geqslant 1$ (percentage difference increases as y decreases). For PIV, differences are less than 3% for $y\geqslant 1$ (this also increases as y decreases). LDA results could be obtained as close as $y=0.05$, while PIV can only be obtained as close as $y=0.19$. LDA and PIV results show the same trend for the two frequencies as predicted by the theory.

The LDA and PIV techniques have some general advantages over the HWA; they are quasinonintrusives, do not require calibration, and distinguish between the signs of the velocity. Nevertheless, for the measurements of oscillatory flows, the frequency that can be resolved by LDA and PIV is limited by the number of seeding particles. However, for these kind of measurements the HWA technique has shown to be able to solve frequencies up to 10 kHz, but for LAVBL measurements the results have presented deviations that depend on the oscillation frequency [11].

VII. CONCLUSIONS

Measurements of the velocity amplitude and phase as a function of distance to the wall in the laminar oscillatory viscous boundary layer produced by acoustic waves were carried out using LDA and PIV techniques. The results agree with Rayleigh and Tominaga's theoretical predictions confirming the existence of a local maximum of the velocity amplitude at approximately $2.4\delta_v$. Consequently, the frequency dependence found in HWA results (presented in [11]) are not intrinsic to the experimental conditions but are due to the interaction between the HWA probe and the wall. LDA and PIV results are consistent each other, but LDA measurements have less experimental uncertainty than PIV, and it allows to perform measurements close to the wall.

ACKNOWLEDGMENTS

This work was supported by CONACyT U41347-F and DGAPA IN104702-2 projects. The authors wish to thank Raúl Rechtman for interesting discussions and Guillermo Hernández for his technical support.

[1] J. W. S. Rayleigh, *The Theory of Sound, Vol. 2* (Dover, New York, 1945).
[2] P. J. Westervelt, J. Acoust. Soc. Am. **25**, 60 (1953).
[3] W. L. Nyborg, *Physical Acoustics*, edited by W. Mason, Vol. IIB (Academic, New York, 1965).
[4] J. Lighthill, J. Sound Vib. **61**, 391 (1978).
[5] Q. Qi, J. Acoust. Soc. Am. **95**, 556 (1993).
[6] S. Cuevas and G. Huelsz, *Recent Research Developments in*

Fluid Dynamics 2 (Pandalai, India, 1999).
[7] G. W. Swift, Phys. Today **48**, 22 (1995).
[8] M. Bruneau, C. Garing, and H. Leblond, J. Acoust. Soc. Am. **80**, 672 (1986).
[9] D. P. Telionis, *Unsteady Viscous Flows* (Springer, New York, 1981).
[10] M. Hino, M. Sawamoto, and S. Takasu, J. Fluid Mech. **75**, 193 (1976).
[11] G. Huelsz, F. López-Alquicira, and E. Ramos, Exp. Fluids **32**, 66 (2002).
[12] R. J. Adrian, *Laser Velocimetry, in Fluids Mechanics Measurements* (Hemisphere Publishing, New York, 1983).
[13] D. Mouazé and P. M. Bélorgey, Exp. Fluids **30**, 111 (2001).
[14] J. H. M. Fransson and K. J. A. Westin, Exp. Fluids **32**, 413 (2002).
[15] D. Poggi, A. Porporato, and L. Ridolfi, Exp. Fluids **32**, 366 (2002).
[16] M. Fischer, M. Raffel, A. Vogt, and J. Kompenhans, Opt. Eng. **33**, 1343 (1994).
[17] C. J. Kahler, Exp. Fluids **36**, 114 (2004).
[18] J. L. Lara, E. A. Cowen, and I. M. Sou, Exp. Fluids **33**, 47 (2002).
[19] T. Loizeau and Y. Gervais, Acust. Acta Acust. **83**, 945 (1997).
[20] H. Bailliet, P. Lotton, M. Bruneau, V. Gusev, J. C. Valiere, and B. Gazengel, Appl. Acoust. **60**, 1 (2000).
[21] J. P. Sharpe, C. A. Greated, C. Gray, and D. M. Campbell, Acustica **68**, 168 (1989).
[22] M. P. Arroyo and C. A. Greated, Meas. Sci. Technol. **2**, 1181 (1991).
[23] D. B. Hann and C. A. Greated, Meas. Sci. Technol. **8**, 1517 (1997).
[24] J. A. Cosgrove, J. M. Buick, S. D. Pye, and C. A. Greated, Ultrasonics **39**, 461 (2001).
[25] M. Campbell, J. A. Cosgrove, C. A. Greated, S. Jack, and D. Rockliff, Opt. Laser Technol. **32**, 629 (2000).
[26] A. Tominaga, Cryogenics **35**, 427 (1995).
[27] A. A. Castrejón-Pita, J. R. Castrejón-Pita, and G. Huelsz, Fractals **11**, 169 (2003).
[28] D. C. Weinert, T. Clearly, and G. W. Mulholland, *AUBE 2001, 12th International Conference on Automatic Fire Detection, Proceedings NIST* (Gaithersbrug, MD, 2001).
[29] W. H. Press, S. A. Teukolsky, W. T. Vetterling, and B. P. Flannery, *Numerical Recipes in C++* (Cambridge University Press, New York, 2002).
[30] M. Ohmi and M. Iguchi, Bull. JSME **25**, 200 (1982).